Comparison of spatial filter selectivity in surface myoelectric signal detection – Influence of the volume conductor model

Medical & Biological Engineering & Computing

COMPARISON OF SPATIAL FILTER SELECTIVITY IN SURFACE MYOELECTRIC SIGNAL DETECTION – INFLUENCE OF THE VOLUME CONDUCTOR MODEL

Dario Farina, Luca Mesin, Simone Martina, Roberto Merletti

Centro di Bioingegneria, Dip. di Elettronica, Politecnico di Torino, Torino, Italy

Keywords: electromyography, EMG modeling, spatial filters, selectivity, end-of-fiber components

Running title: Volume conductor model and spatial selectivity

Corresponding author:

Dario Farina, PhD

Dipartimento di Elettronica, Politecnico di Torino; Corso Duca degli Abruzzi 24, Torino, 10129 ITALY

Tel. 0039-0114330476; Fax. 0039-0114330404; e-mail : dario.farina@polito.it

Acknowledgements

This work was supported by the European Shared Cost Project *Neuromuscular assessment in the Elderly Worker* (NEW) (Contract n° QLRT-2000-00139).

ABSTRACT

Spatial filters are used for increasing selectivity in surface EMG signal detection. This study investigated the importance of the description of the volume conductor for inferring conclusions on comparing filter selectivity from simulation analyses. A cylindrical multi-layer description of the volume conductor was used for the simulation analysis. Different anatomies were analyzed with this model and results on filter selectivity compared. The longitudinal single (LSD), double (LDD) and normal double differential (Laplacian, NDD) filters were investigated. Largely different conclusions could be drawn when comparing filter selectivity resulting from simulations with different volume conductor models. A filter which performed best with a particular anatomy could be the poorest with another anatomy. While with a bone/muscle model and superficial fibers, the ratio between peak-to-peak values of the propagating and non-propagating signal components was approximately 220% for LDD and LSD and lower than for NDD (approximately 290%), with a bone/muscle/fat/skin model LSD performed significantly worse (150%) than both LDD and NDD, which showed similar performance (approximately 300%). Similarly, increasing the lateral distance of the recording by 10°, signal amplitude was reduced to 2% with LSD and LDD and to 4% with NDD. With another anatomy, LSD and LDD reduced signal amplitude to 20-25% while NDD reduced it to 4%. Similar considerations could be drawn for other selectivity indexes. Thus, modeling should be used carefully to infer conclusions on spatial selectivity and to indicate particular selections of spatial filters.

1. INTRODUCTION

During voluntary muscle contractions, the electrical activity of the active motor units (MUs) may be detected by electrodes placed over the skin. The resultant surface electromyographic (EMG) signal is termed interference since the contributions of the MUs are superimposed and difficult to separate. The tissues interposed between the signal sources and the detection electrodes indeed act as low-pass filters, causing a blurring effect on the surface potentials. The electrical potential generated by a source is thus spread in a large region over the skin. The sources are poorly localized in space with the consequence that many sources contribute to the signal generated at the detection location.

As in image processing, spatial selectivity can be enhanced by proper signal filtering. Since the volume conductor can be described as a spatial low-pass filter (LINDSTROM and MAGNUSSON, 1977; STEGEMAN *et al.,* 2000), a high-pass filtering in the spatial domain may be used to counteract the blurring effect of the tissues. As high-pass filters enhance the edges in image processing, in the case of surface EMG detection, spatial high-pass filters may reduce the spatial spread of the surface potentials, thus allowing better localization of the sources.

In surface EMG, spatial filtering is performed by the weighted summation of signals detected by electrodes arranged in particular geometrical configurations. A bipolar recording can be described by a sinusoidal transfer function in the spatial frequency domain (LINDSTROM and MAGNUSSON, 1977), thus it is a high-pass spatial filter for signals with spatial bandwidth smaller than half of the inverse of the inter-electrode distance. The same can be done for more complex configurations of point (REUCHER *et al.,* 1987; REUCHER *et al.*, 1987; DISSELHORST-KLUG *et al.*, 1997) or non-point (FARINA and CESCON, 2001) electrodes. The detection of surface EMG by two-dimensional (2-D) configurations of electrodes, representing selective high-pass spatial filters in a limited bandwidth, has been termed as high spatial resolution EMG (HSR-EMG) (RAU and DISSELHORST-KLUG, 1997), to indicate the high selectivity of these recording systems. Although not as widespread as the classic bipolar recordings, 2-D spatial filters have been recently applied by many research groups for single MU studies (HOGREL and DUCHENE, 1999; HUPPERTZ *et al.,* 1997; RAMAEKERS *et al.,* 1993).

Given the extensive use of spatial filtering in recent EMG studies, comparison of selectivity of these systems is an important issue. Indeed, theoretically highly selective spatial filters are usually comprised of more detection surfaces than less selective ones (REUCHER *et al.*, 1987a; REUCHER *et al.*, 1987b). Signal detection is thus more complex in the case of HSR-EMG than for classic bipolar recordings. For establishing if complex systems are worth to be used instead of classic ones, it is necessary to quantify the gain in terms of spatial selectivity obtained at the expenses of a more complex detection modality.

Spatial selectivity should be interpreted as selectivity with respect to propagating and non-propagating signal components (FARINA *et al.*, 2002a; FARINA *et al.*, 2002b; DIMITROVA *et al.*, 2002). The former are generated by the intra-cellular action potential (IAP) traveling along the muscle fibers, the latter are due to the generation and extinction of the IAP at the end-plates and tendon junctions. A system may be more selective than another with respect to a specific component and not for another signal component. For example, experimental results on leg muscles showed that, among a number of one-dimensional (1-D) and two-dimensional (2-D) detection systems, the longitudinal double differential filter is the most selective for cross-talk signals (DISSELHORST-KLUG *et al.*, 1999; VAN VUGT and VAN DIJK, 2001), while more isotropic filters, such as the Laplacian, are best with respect to propagating components (FARINA *et al.*, 2003a; FARINA *et al.*, 2003b).

Selectivity to propagating signal components is related to the feasibility of detecting single MU activities (RAU and DISSELHORST-KLUG,1997) since propagating components are dominant in case of sources close to the detection point. On the other hand, the ability to reduce non-propagating signals is important for crosstalk since crosstalk is mainly due to these signal components (FARINA *et al.*, 2002b). Moreover, a better reduction of non-propagating signals implies a lower bias of conduction velocity estimates (FARINA *et al.*, 2002a).

There are a few studies reporting comparison of spatial filters for surface EMG detection. Comparison of selectivity can be achieved by 1) theoretical considerations (GYDIKOV *et al.*, 1986),

2) surface EMG signal modeling (DIMITROV *et al.*, 2003), or 3) experimental observations (DISSELHORST-KLUG *et al.*, 1997; FARINA *et al.*, 2003a; FARINA *et al.*, 2003b; VAN VUGT and VAN DIJK, 2001). The first approach is based on the comparison of spatial filter transfer functions and theoretical up-take areas or volumes and provide indications whose validity is limited to simplified conditions which may be far from practice. Modeling allows investigation of a large range of conditions which is often not possible in experimental analyses. However, a model is still a simplified description of the actual surface EMG generation and detection system and conclusions reached by modeling should be considered carefully. The experimental approach is preferable to the modeling one but may be difficult to perform for obvious technical difficulties.

It has been shown that different volume conductor models may lead to different results in terms of decrease of monopolar potential amplitude with distance from the source (ROELEVELD *et al.*, 1997). In particular, it is well known that adding subcutaneous layers in addition to the muscle tissue in a model results in larger spread of the surface potential distribution (e.g., FARINA and RAINOLDI, 1999). This is due to both the increased distance of the sources with respect to the detection points and the different conductivity properties of the subcutaneous layers with respect to the muscle tissue (ROELEVELD *et al.*, 1997).

Relative comparison of selectivity of spatial filters, that is the analysis of which filters are more or less selective with respect to others, may also be affected by the use of different simulation models, in particular of different anatomical conditions. This is due to the different characteristics of the muscle tissue (anisotropic) with respect to subcutaneous layers (isotropic). Different filters, in particular highly anisotropic versus almost isotropic ones, may be more or less sensitive to the anatomy. Thus, a filter more selective than another for a certain volume conductor description may be less selective when applied to another description. These issues should be considered in simulation studies which aim at investigating differences in selectivity of spatial filters and/or at proposing new filters on the basis of a simulation-based validation of performance.

The hypothesis tested in the present simulation study is that adding subcutaneous layers to the volume conductor may lead to different conclusions on relative comparison of selectivity of spatial filters to both propagating and non-propagating signal components.

2. METHODS

2.1 Simulation model

The analytical model used describes the volume conductor as a cylindrical layered medium (BLOK *et al.*, 2002; GOOTZEN *et al.*, 1991) and has been implemented as described by Farina *et al.* (2003c). Different numbers of tissue layers may be included. We analyzed three sets of layers, corresponding to a volume conductor comprised of 1) bone and muscle, 2) bone, muscle, and fat, 3) bone, muscle, fat, and skin (Figure 1). The conductivity of the bone was set to 0.02 S/m, that of the muscle was 0.5 S/m in the fiber direction and 0.1 S/m in the transverse directions, that of the fat layer was 0.05 S/m, and that of the skin varied among 0.1 S/m, 0.5 S/m, and 1 S/m. Fat layer thickness varied among 1 mm, 3 mm, and 5 mm. In total, the latter choices led to 13 volume conductor descriptions (Table I). The 13 configurations have been compared in the case of muscle fibers located at the same depth within the muscle (Figure 1).

Table I and Figure 1 about here

The model accounts for the generation, propagation, and extinction of the IAPs at the end-plate, along the fiber, and at the tendons, respectively. These phenomena are described by the progressive generation, propagation, and extinction of the first derivative of the IAP (DIMITROV and DIMITROVA, 1998; FARINA and MERLETTI, 2001; FARINA *et al.*, 2003c). The IAP shape was described as proposed by ROSENFALCK (1969). Point electrodes were considered in all cases and only single fiber action potentials were simulated. The simulated conduction velocity was 4 m/s.

2.2 Spatial filters and indexes of selectivity

The analyzed spatial filters were the longitudinal single and double differential (LSD and LDD) and the normal double differential (NDD) (Figure 1c). Inter-electrode distance was 5 mm in the results shown, although the simulations were performed also for 10 mm inter-electrode distance.

Selectivity was evaluated in the longitudinal and transverse directions with respect to muscle fiber orientation and in the depth direction. Signals were simulated as detected at different transverse distances from fibers located at different depths (Figure 1). The selectivity indexes were defined as the percent ratio between the peak-to-peak signal components for depths of the fiber of 5 mm and 1 mm within the muscle, and for transverse distances of 10 degrees and 0 degrees with respect to the detection system. It is clear that there are many alternative ways of defining selectivity indexes other than the previous definitions. We decided to compare the initial amplitude decrease (for short distances) since similar indexes have been used for assessing transverse selectivity in recent experimental studies (FARINA *et al.*, 2003b). The more selective the detection system, the higher the amplitude decrease. In particular, we will compare in the following the percent of signal amplitude from a deeper source with respect to a more superficial one (depth selectivity, DS) and the percent of signal amplitude from a transversally distant source with respect to a source located under the detection system (transverse selectivity, TS). Smaller percentages of signal amplitude generated by sources more far away with respect to closer sources will indicate higher selectivity of the detection system.

We defined the interval of time T_p with "propagating" signal component as that corresponding to the generation and propagation of the IAP; non-propagating signals corresponded to the interval of time during which the IAP extinguished at the tendon junctions. With the above definition, the "propagating" component does not travel without shape changes because of the effect of the end-plate and of the traveling of the IAP along the opposite fiber semi-length. Being aware of this ambiguous definition, we will refer in the following to propagating signal component as the part of

the signal corresponding to IAP generation and traveling. The selectivity indexes will be reported for both the propagating and the non-propagating signal components.

Longitudinal selectivity was evaluated by the temporal support of the simulated potentials, defined as the square root of the normalized second order central moment of $x^2(t)$, as indicated below:

$$B_t = \sqrt{\frac{\int_0^T \left(t-\bar{t}\right)^2 x^2(t)\mathrm{d}t}{\int_0^T x^2(t)\mathrm{d}t}}$$
$$\bar{t} = \frac{\int_0^T t x^2(t)\mathrm{d}t}{\int_0^T x^2(t)\mathrm{d}t} \qquad (1)$$

where T is the total time interval in which the signal $x(t)$ is simulated. With respect to other definitions of duration, B_t has a resolution not limited by the sampling period. The smaller B_t, the more selective the filter. It has to be noted that B_t may assume much smaller values than other indexes of time duration, such as those based on a high fraction of signal energy contained within a certain interval of time. As for the other selectivity indexes, alternative definitions are possible. These choices are not critical for the results shown in this study.

3. RESULTS

Figure 2 shows representative potentials simulated at different transverse distances (at steps of 2.5 degrees, corresponding to 2.18 mm for a radius of 50 mm) from the fiber and detected by the LDD and the NDD systems. Two anatomies have been simulated in this example. The signals detected by both filters are affected by the anatomy selected. NDD signals show an inversion of polarity which is due to the geometrical relations between the electrodes and the fiber. This inversion is clearly visible with one anatomy but not with the other. It is also evident that the difference in signal attenuation with distance between the two filters is more pronounced with one anatomy than with the other.

Figure 2 about here

3.1 Relative weight of propagating and non-propagating signal components

Figure 3 reports the ratio (PNP) between propagating and non-propagating signal components for the 13 anatomies, the three spatial filters, and two angles of inclination (0 and 15 degrees) of the recording systems with respect to the muscle fiber orientation. A short semi-fiber length (30 mm) has been selected for representative purposes. Note that in this case the relative weight of non-propagating components is rather large.

Considering, e.g., results from the first anatomy, in case of superficial fibers, the LDD and LSD recordings show similar PNP, lower than with NDD. The differences are rather large. With other anatomies the situation changes significantly. With bone, muscle, fat, and a highly conductive skin layer, LSD shows PNP significantly lower than LDD (approximately 160% versus approximately 280%) with NDD still showing higher PNP. Increasing the fat layer thickness and decreasing skin conductivity, LDD and NDD perform similarly with LSD leading to significantly smaller PNP (150% versus 300%).

Increasing fiber depth (Figure 3b), in average, PNP is lower than for superficial fibers, as expected. In this case, LDD leads to significantly higher PNP than NDD with all the anatomies. However, LSD may be significantly worse or better than both LDD and NDD, depending on the description of the volume conductor. Again the differences are quite large. While with a bone/muscle model, LSD performs worse than the other two filters (PNP approximately 150% versus PNP higher than 200%), with other anatomies it performs best.

Figure 3 about here

3.2 Selectivity in depth direction

Figure 4a reports the percent amplitude of the propagating component of the signal with depth of the fiber 5 mm with respect to that obtained from a fiber at 1 mm within the muscle. Results from

the 13 anatomies, the three spatial filters, and two angles of inclination (0 and 15 degrees) of the recording systems with respect to the muscle fiber orientation are reported. As expected, the anatomy influences results with a general decrease of selectivity when isotropic layers are added. The relative performance of the different filters is not much affected by the anatomy. On the contrary, when investigating the selectivity with respect to end-of-fiber components (Figure 4b), the anatomy selected leads to different conclusions on the relative comparison of filter selectivity. NDD is in general less selective with respect to these components than LDD and LSD, although the difference depends on the anatomy. LSD may be more or less selective than LDD depending on the description of the volume conductor (compare, e.g., anatomies 5, 7, and 11).

Figure 4 about here

3.3 Selectivity in transverse direction

The effect of the anatomy on the percent of signal amplitude with increasing transverse distance by 10 degrees with respect to the amplitude obtained from a fiber under the detection system is large (Figure 5). Both in case of propagating and non-propagating signal components, relative behavior of spatial filters is highly influenced by the anatomy. LSD, LDD, and NDD show similar performance with some anatomies (e.g., the first) while they perform significantly differently with other anatomies (e.g., the 11^{th}). The differences are not negligible and important for practical applications. With the fifth anatomy, for example, when lateral displacement of the detection system increases from 0° to 10°, the propagating components are reduced to approximately 2% with LSD and LDD and to approximately 4% with NDD. With the 11^{th} anatomy, LSD and LDD reduce the signal amplitude to approximately 25% and 20% respectively, while with NDD amplitude decreases to 4%. Similar considerations hold for the non-propagating part of the signal (Figure 5b).

Figure 5 about here

3.4 Selectivity in longitudinal direction

As for the other selectivity indexes, also longitudinal selectivity is affected by the volume conductor description (Figure 6). Comparison of spatial filters depends on the anatomy. In general, the action potentials are longer when tissue layers are added, as expected. For superficial fibers (Figure 6a), LDD potentials have longer duration than NDD and LSD in case of the bone/muscle model, while LSD shows longer potentials than the other two filters for other volume conductor descriptions. Increasing fiber depth (Figure 6b), the duration of the potentials increases, as expected. In this case, LSD shows always longer potentials than the other two filters.

Figure 6 about here

4. DISCUSSION

Roeleveld *et al.* (1997) indicated that complex volume conductors are needed for EMG signal simulation when interpreting experimental results. These authors showed that experimental monopolar data could not be matched with simple models while they could be explained by more complex simulation approaches. The presence of subcutaneous layers increases the geometrical distance between the muscle fibers and the detecting electrodes, thus increasing the spread of the potential distribution over the detection surface. In addition, the combination of isotropic and anisotropic layers may increase the spatial distribution of the surface potentials more than expected by simple depth increase (ROELEVELD *et al.*, 1997; STEGEMAN *et al.*, 2000). The hypothesis to be tested in the present work was that the spatial potential spread over the detection surface may be influenced by the volume conductor in different ways depending on the spatial filter applied for the detection. Thus, relative comparisons of different filters by simulations strongly depends on the model used. In terms of selectivity, one filter may be better than another with one volume conductor description while the opposite may happen with another description. The addition of isotropic layers

makes the volume conductor transfer function more isotropic than with muscle only. This is especially true for superficial fibers. Highly anisotropic and almost isotropic spatial filters may thus have different effects for different volume conductor models. Differences in relative comparison of spatial filters may probably be obtained also with simpler ways of describing subcutaneous layers, e.g., by increasing source depth within the muscle. In the latter case, the volume conductor transfer function changes due to depth without the effect of isotropic transfer functions. The results would still be different from those reported in this study, showing the large sensitivity of the conclusions to the model used. Moreover, other generation and detection system parameters may have an influence on the results. Changing inter-electrode distance, for example, scales the theoretical transfer function of the spatial filters. Depending on the inter-electrode distance, it is also possible that the spatial bandwidth of the signal is larger than the period of repetition, in the spatial frequency domain, of the transfer function of the spatial filter. The same simulations shown in this study were repeated with 10 mm inter-electrode distance (results not shown) and the general conclusion was of a large effect of the volume conductor on the comparison of the filters, as for the case of 5 mm.

Selectivity should be evaluated in depth, transverse, and longitudinal direction for both propagating and non-propagating components. A simulation study on the issue of selectivity is very complex since the factors to be considered are many. Both the model used for the simulations and the number of conditions simulated are important.

The previous observations lead to the considerations that 1) in practical applications improvement of spatial selectivity by complex spatial filters may be more or less pronounced (or may even be absent) depending on the muscle and subject analyzed (i.e., on the anatomy), and 2) modeling should be carefully used to infer conclusions on spatial selectivity and to indicate particular selections of spatial filters.

Simplified descriptions of the volume conductor provide significantly different conclusions on spatial filter selectivity than more complex descriptions. It is doubtless that other volume conductor

models (e.g., planar, FARINA and MERLETTI, 2001) with respect to those analyzed in this study would lead to still different results and different conclusions on the comparison of spatial filters. Indications limited to a particular aspect of spatial selectivity and obtained with simple models may thus be confusing since may not cover all the aspects important for filter comparison. A model can not reproduce the real muscle anatomy in practical measures; even considering simplifications, such as layered volume conductors, it is not possible to measure and introduce exactly in the model some important parameters, such as conductivity of the layers. Moreover, the model used in this study assumes homogeneous bone, muscle, fat, and skin layers with sharp borders. In real situations the edges are not sharp and a number of other tissues (blood vessels, glands, etc.) make the media rather dishomogeneous, likely altering the shape of the surface motor unit action potentials. All these parameters play a role not only on the monopolar potential spread over the skin but also on the relative comparison of selectivity of spatial filters. Thus, interpretation of experimental results on selectivity by modeling is very critical. Suggestions on spatial filter selection by a modeling approach leads clearly to even greater problems.

The differences in spatial selectivity and reduction of end-of-fiber components for different anatomies observed in this study were rather large. When addressing the ratio between propagating and non-propagating signal components for superficial fibers, we obtained values between 150% and 350% for LSD, LDD, and NDD, depending on the volume conductor description. The difference between LDD and NDD with a bone/muscle model was reduced with other models (Figure 3). Experimental results showing a similar bias in single MU conduction velocity estimates when signals are collected by LDD and NDD (SCHULTE *et al.*, 2003) are in agreement with the present simulation results in case of some anatomies but not with others. Since optimal reduction of non-propagating components is reached by different filters depending on the anatomical condition, estimation of conduction velocity may be improved by adaptive selection of the spatial filters for signal detection (FARINA and MERLETTI, 2003).

As for the ratio between propagating and non-propagating signal components, the selectivity of individual spatial filters is highly dependent on the description of the volume conductor. Transverse selectivity is, in particular, largely affected by the tissues interposed between the muscle fibers and the electrodes. The improvement in spatial selectivity by 2-D recordings with respect to 1-D ones is more or less pronounced depending on the volume conductor. A bone/muscle model predicts a similar transverse selectivity of LDD and LSD with respect to NDD. With other anatomies, 1-D systems are even more selective than the 2-D one. The latter observation is not in agreement with experimental results on tibialis anterior, biceps brachii, and upper trapezius muscles (FARINA *et al.*, 2003a; FARINA *et al.*, 2003b). For these muscles it was indeed shown that NDD significantly increased selectivity of the recordings in the transverse direction with respect to LDD. Anatomical descriptions more complex than the bone/muscle may explain these experimental results.

5. CONCLUSIONS

Relative performance of spatial filter selectivity largely depends on the anatomy. A spatial filter may be more or less selective than another depending on the volume conductor description. With different models or adding layers of different conductivities to the same description of the volume conductor (e.g., layered with circular symmetry), one filter may be best among others while it may be the worst with other volume conductor structures. Since the real surface EMG generation and detection system is more complex than any model, this variability of results with different models is critical and indicates that modeling should be carefully used when addressing the issue of spatial filter selectivity. This is in general true for many other issues which may be investigated by modeling. For issues in which the description of the volume conductor is critical, the experimental paradigm should be used rather than or in addition to modeling. Practical indications provided by modeling about the optimal filter to use are inherently limited. For the same reasons, the proposal of new filters should be accompanied by an experimental validation rather than or in addition to a simulation-based test of performance.

Thus, the main conclusion of this study is that the description of the volume conductor significantly affects the relative comparison of spatial filter selectivity in simulation analysis. Results on selectivity obtained with models should be considered with caution when discussing practical applications.

REFERENCES

1. BLOK, J.H., STEGEMAN, D.F., and VAN OOSTEROM A. (2002): 'Three-layer volume conductor model and software package for applications in surface electromyography', *Ann. Biomed. Eng.*, **30**, pp. 566-577
2. DIMITROV, G.V., and DIMITROVA, N.A. (1998): 'Precise and fast calculation of the motor unit potentials detected by a point and rectangular plate electrode', *Med. Eng. & Phys.*, **20**, pp. 374-381
3. DIMITROV, G.V., DISSELHORST-KLUG, C., DIMITROVA, N.A., SCHULTE, E., and RAU, G. (2003): 'Simulation analysis of the ability of different types of multi-electrodes to increase selectivity of detection and to reduce cross-talk'. *J. Electromyogr. Kinesiol*., **13**, pp. 125 – 138
4. DIMITROVA, N.A., DIMITROV, G.V., and NIKITIN, O.A. (2002): 'Neither high-pass filtering nor mathematical differentiation of the EMG signals can considerably reduce cross-talk'. *J. Electromyogr. Kinesiol.*, **12**, pp. 235 – 246
5. DISSELHORST-KLUG, C., SILNY, J., and RAU, G. (1997): 'Improvement of spatial resolution in surface-EMG: a theoretical and experimental comparison of different spatial filters'. *IEEE Trans. Biomed. Eng.*, **44**, pp. 567 – 574
6. DISSELHORST-KLUG, C., BLANC, Y., and RAU, G. (1999): 'Examination of the reduction of crosstalk between the leg muscles by spatial filtering techniques'. Results of small SENIAM projects, chapter 1, pp. 38 – 40
7. FARINA, D., and MERLETTI, R. (2001): 'A novel approach for precise simulation of the EMG signal detected by surface electrodes'. *IEEE Trans. Biomed. Eng.*, **48**, pp. 637 – 646
8. FARINA, D., and CESCON, C. (2001): 'Concentric ring electrode systems for non-invasive detection of single motor unit activity'. *IEEE Trans. Biomed. Eng.*, **48**, pp. 1326 – 1334
9. FARINA, D., CESCON, C., and MERLETTI, R. (2002a): 'Influence of anatomical, physical and detection-system parameters on surface EMG'. *Biol. Cybern.*, **86**, pp. 445 – 456

10. FARINA, D., MERLETTI, R., INDINO, B., NAZZARO, M., and POZZO, M. (2002b): 'Cross-talk between knee extensor muscles. Experimental and modelling results'. *Muscle & Nerve*, **26**, pp. 681 – 95

11. FARINA, D., ARENDT-NIELSEN, L., MERLETTI, R., INDINO, B., and GRAVEN-NIELSEN, T. (2003a): 'Selectivity of spatial filters for surface EMG detection from the tibialis anterior muscle'. *IEEE Trans. Biomed. Eng.*, **50**, pp. 354 – 364

12. FARINA, D., SCHULTE, E., MERLETTI, R., RAU, G., and DISSELHORST-KLUG, C. (2003b): 'Single motor unit analysis from spatially filtered surface EMG signals – Part I : spatial selectivity', *Med. Biol. Eng. Comput.*, **41**, pp. 330-7

13. FARINA, D., and MERLETTI, R. (2003): 'A novel approach for estimating muscle fiber conduction velocity by spatial and temporal filtering of surface EMG signals', *IEEE Trans. Biomed. Eng.*, in press

14. FARINA, D., MESIN, L., MARTINA, S., and MERLETTI, R. (2003c): 'A new surface EMG generation model with multi-layer cylindrical description of the volume conductor', *IEEE Trans. Biomed. Eng.*, in press

15. GOOTZEN, T.H., STEGEMAN, D.F., and VAN OOSTEROM, A. (1991): 'Finite limb dimensions and finite muscle length in a model for the generation of electromyographic signals', *Electroenc. Clin. Neurophysiol.*, **81**, pp. 152-162

16. GYDIKOV, A., KOSSEV, A., TRAYANOVA, N., RADICHEVA, N. (1986): 'Selective recording of motor unit potentials'. *Electromyogr. Clin. Neurophysiol*., **26**, pp. 273 – 281

17. HOGREL, J.Y., and DUCHÊNE, J. (1999): 'A sEMG-based system for clinical applications using laplacian electrodes'. Proc. of the 4th General SENIAM Workshop, The Netherlands, pp. 172 – 177

18. HUPPERTZ, H.J., DISSELHORST-KLUG, C., SILNY, J., RAU, G., and HEIMANN, G. (1997): 'Diagnostic yield of noninvasive High-Spatial-Resolution-EMG in Neuromuscular Disease', *Muscle & Nerve*, **20**, pp. 1360 – 1370

19. LINDSTROM, L., and MAGNUSSON, R. (1977): 'Interpretation of myoelectric power spectra: a model and its applications', *Proc. IEEE*, **65**, pp. 653 – 662

20. RAMAEKERS, V.T., DISSELHORST-KLUG, C., SCHNEIDER, J., SILNY, J., FORST, J., FORST, R., KOTLAREK, F., and RAU, G. (1993): 'Clinical application of a noninvasive multi-electrode array EMG for the recording of single motor unit activity'. *Neuropediatrics.*, **24**, pp**.** 134 – 8

21. RAU, G., and DISSELHORST-KLUG, C. (1997): 'Principles of high-spatial-resolution surface EMG (HSR-EMG): single motor unit detection and application in the diagnosis of neuromuscular disorders'. *J. Electromyogr. Kinesiol*., **7**, pp. 233 – 239

22. REUCHER, H., RAU, G., and SILNY, J. (1987a): 'Spatial filtering of noninvasive multielectrode EMG: Part I--Introduction to measuring technique and applications'. *IEEE Trans. Biomed. Eng.*, **34**, pp. 98 – 105

23. REUCHER, H., SILNY, J., and RAU, G. (1987b): 'Spatial filtering of noninvasive multielectrode EMG: Part II--Filter performance in theory and modeling', *IEEE Trans. Biomed. Eng.*, **34**, pp. 106 – 113

24. ROELEVELD, K., BLOK, J.H., STEGEMAN, D.F., and VAN OOSTEROM, A. (1997): 'Volume conduction models for surface EMG; confrontation with measurements'. *J. Electromyogr. Kinesiol.*, **7**, pp. 221 – 232

25. ROSENFALCK, P. (1969): 'Intra and extracellular fields of active nerve and muscle fibers. A physico-mathematical analysis of different models', *Acta Physiol. Scand.*, **321**, pp. 1-49

26. SCHULTE, E., FARINA, D., RAU, G., MERLETTI, R., and DISSELHORST-KLUG, C. (2003): 'Single motor unit analysis from spatially filtered surface EMG signals – Part II : conduction velocity estimation', *Med. Biol. Eng. Comput.*, **41**, pp. 338-45

27. STEGEMAN, D.F., BLOK, J.H., HERMENS, H.J., and ROELEVELD, K. (2000): 'Surface EMG models: properties and applications'. *J. Electromyogr. Kinesiol.*, **10**, pp. 313 – 26

28. VAN VUGT, J.P.P., VAN DIJK, J.G. (2001): 'A convenient method to reduce crosstalk in surface EMG'. *Clin. Neurophysiol.*, **112**, pp. 583 – 592

TABLE CAPTION

Tab. I The 13 simulated anatomical conditions. The conductivity (indicated by C) and thickness (indicated by Thick; Radius in the case of the bone) of the different layers are reported. VC stands for “Volume conductor”. NP stands for “Not Present” and indicates that the layer was not included in the specific anatomical condition. Summation of the bone radius and the thicknesses of the other layers leads in all cases to 50 mm, which is the radius of the simulated limb fixed for the 13 anatomies. Bone, fat, and skin are isotropic in all cases, thus a single conductivity value is reported. The muscle tissue is anisotropic and two conductivity values are reported, corresponding respectively to conductivity in the radial and angular direction and in the longitudinal direction.

FIGURE CAPTIONS

Fig. 1 a) Section of the volume conductor for three anatomical configurations corresponding to bone/muscle, bone/muscle/fat, and bone/muscle/fat/skin. The muscle fiber is simulated at the same depth within the muscle. b) Lateral view of the volume conductor with the simulate finite-length muscle fiber. Each detection point corresponded to the center of the detection system, which was the central electrode for LDD and NDD and the middle point between the two electrodes for LSD. At the detection point, in this figure, an LSD system is placed, for representative purposes. c) The spatial filters investigated.

Fig. 2 Simulated single fiber action potentials detected at different transverse distances (at steps of 2.5 degrees) from the source and detected by NDD and LDD. Results with two anatomical conditions (corresponding to the 1^{st}, (a), and the 11^{th}, (b), in Table I) are reported. The fiber is at a depth of 1 mm within the muscle in both cases. Fiber semi-length is 50 mm.

Fig. 3 Ratio (PNP) between the peak-to-peak amplitude of the propagating and the non-propagating signal components for a superficial (1 mm within the muscle) (a) and a deeper (5 mm within the muscle) (b) fiber. Fiber semi-length is 30 mm. The cases of an inclination angle of 0 or 15 degrees between the detection system and the muscle fiber are reported. The anatomies reported on the abscissa axis refer to the descriptions provided in Table I.

Fig. 4 Ratio (DS, %) between the peak-to-peak amplitude of the signals generated by fibers at 5 mm and 1 mm depth within the muscle in case of the propagating (a) and the non-propagating (b) part of the potential. Fiber semi-length is 50 mm (a) and 30 mm (b). The cases of an inclination angle of 0 or 15 degrees between the detection system and the muscle fiber are reported. The anatomies reported on the abscissa axis refer to the descriptions provided in Table I.

Fig. 5 Ratio (TS, %) between the peak-to-peak amplitude of signals generated by fibers at 10 degrees and 0 degrees of transverse distance from the detection point. The fiber is 1 mm deep within the muscle. Fiber semi-length is 50 mm (a) and 30 mm (b). The cases of an inclination angle of 0 or 15 degrees between the detection system and the muscle fiber are reported. The anatomies reported on the abscissa axis refer to the descriptions provided in Table I.

Fig. 6 Temporal support (B_t) of the propagating part of the simulated potentials for a superficial (1 mm within the muscle) (a) and a deeper (5 mm within the muscle) (b) fiber. Fiber semi-length is 50 mm. The cases of an inclination angle of 0 or 15 degrees between the detection system and the muscle fiber are reported. The anatomies reported on the abscissa axis refer to the descriptions provided in Table I.

Tab 1

VC model	**Bone** (isotropic)		**Muscle** (anisotropic)		**Fat layer** (isotropic)		**Skin layer** (isotropic)	
	C (S/m)	Radius (mm)	C (S/m)	Thick (mm)	C (S/m)	Thick (mm)	C (S/m)	Thick (mm)
1	0.02	20	0.1; 0.5	30	**NP**	**NP**	**NP**	**NP**
2	0.02	20	0.1; 0.5	29	0.05	1	**NP**	**NP**
3	0.02	20	0.1; 0.5	28	0.05	1	1	1
4	0.02	20	0.1; 0.5	28	0.05	1	0.5	1
5	0.02	20	0.1; 0.5	28	0.05	1	0.1	1
6	0.02	20	0.1; 0.5	27	0.05	3	**NP**	**NP**
7	0.02	20	0.1; 0.5	26	0.05	3	1	1
8	0.02	20	0.1; 0.5	26	0.05	3	0.5	1
9	0.02	20	0.1; 0.5	26	0.05	3	0.1	1
10	0.02	20	0.1; 0.5	25	0.05	5	**NP**	**NP**
11	0.02	20	0.1; 0.5	24	0.05	5	1	1
12	0.02	20	0.1; 0.5	24	0.05	5	0.5	1
13	0.02	20	0.1; 0.5	24	0.05	5	0.1	1

Fig 1

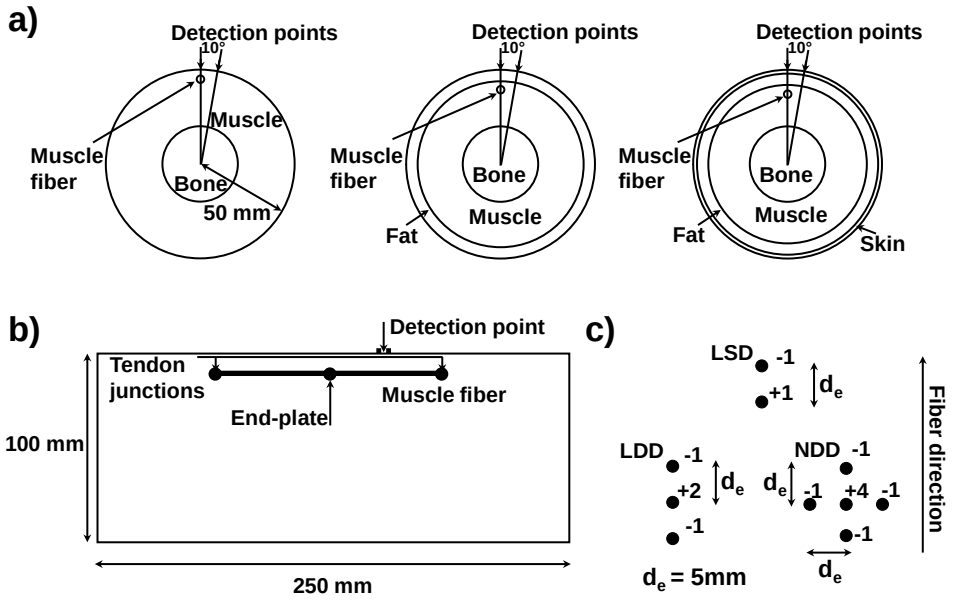
a)
Detection points
10°
Muscle
Muscle fiber
Bone
50 mm
Detection points
10°
Muscle fiber
Bone
Muscle
Fat
Detection points
10°
Muscle fiber
Bone
Muscle
Fat
Skin
b)
Detection point
Tendon junctions
Muscle fiber
End-plate
100 mm
250 mm
c)
LSD
-1
+1
d_e
Fiber direction
LDD
-1
+2
-1
d_e
NDD
-1
d_e
-1
+4
-1
-1
d_e
d_e = 5mm

Fig 2

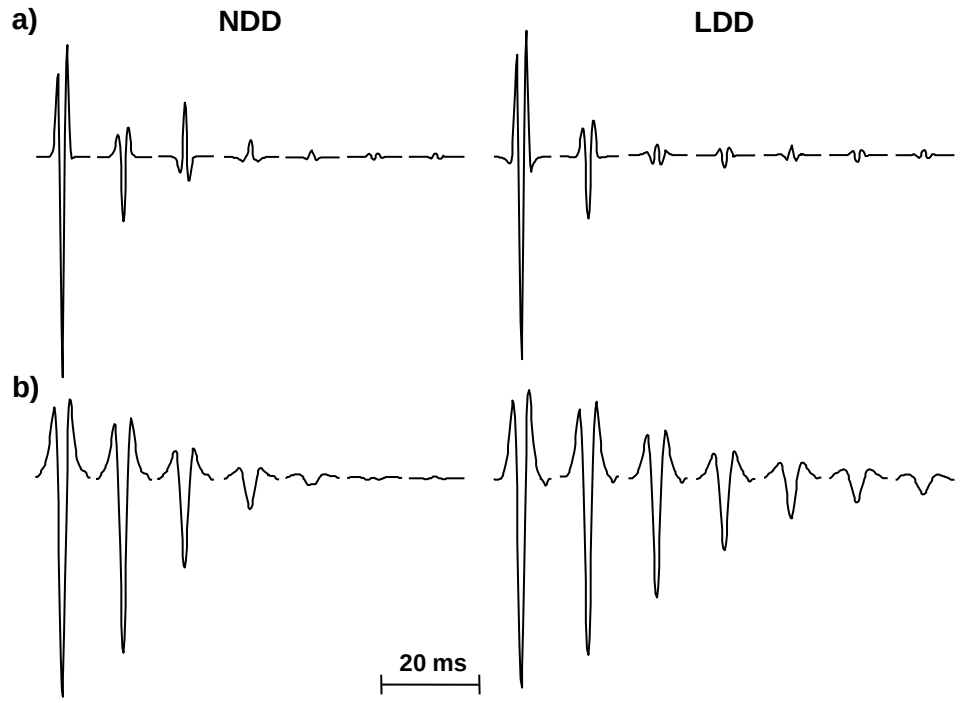
a)
NDD
LDD
b)
20 ms

Fig 3

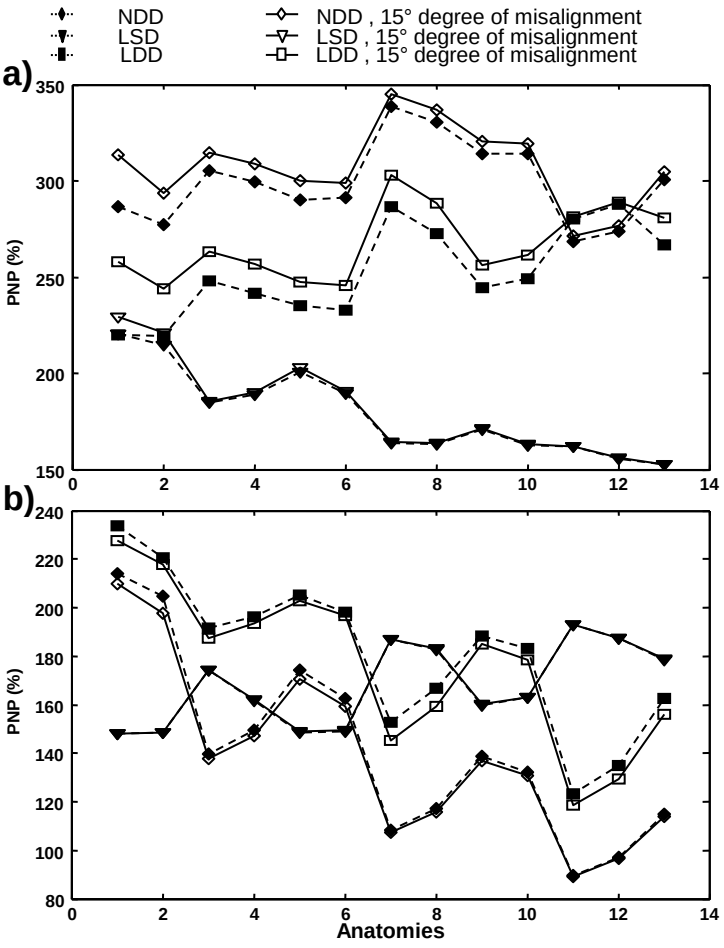
NDD
LSD
LDD
NDD , 15° degree of misalignment
LSD , 15° degree of misalignment
LDD , 15° degree of misalignment
a)
b)
PNP (%)
PNP (%)
Anatomies

Fig 4

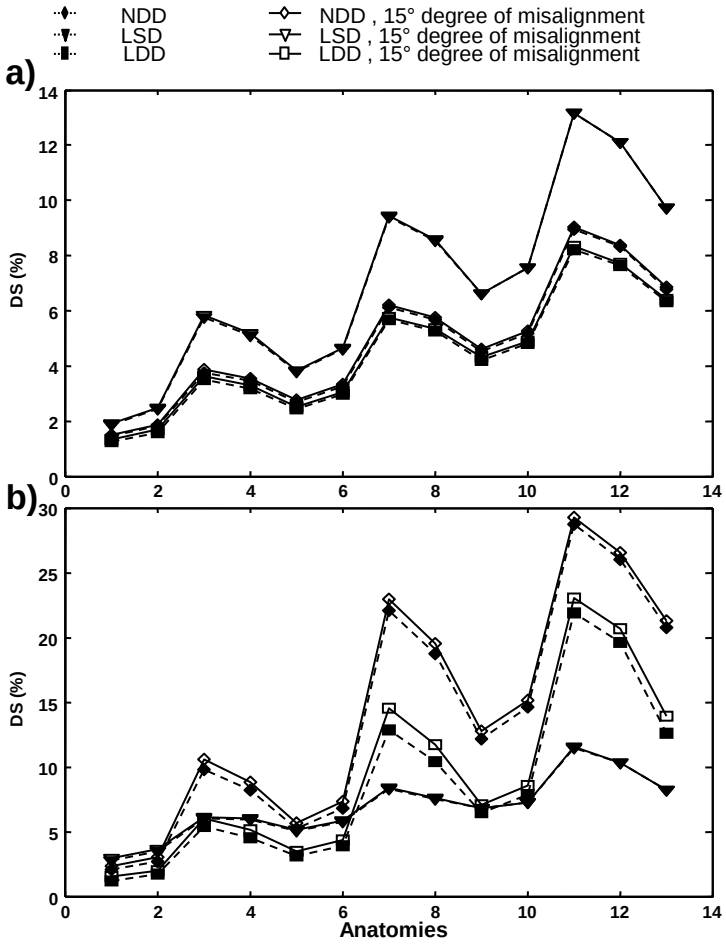
NDD
LSD
LDD
NDD , 15° degree of misalignment
LSD , 15° degree of misalignment
LDD , 15° degree of misalignment
a)
b)
DS (%)
DS (%)
Anatomies

Fig 5

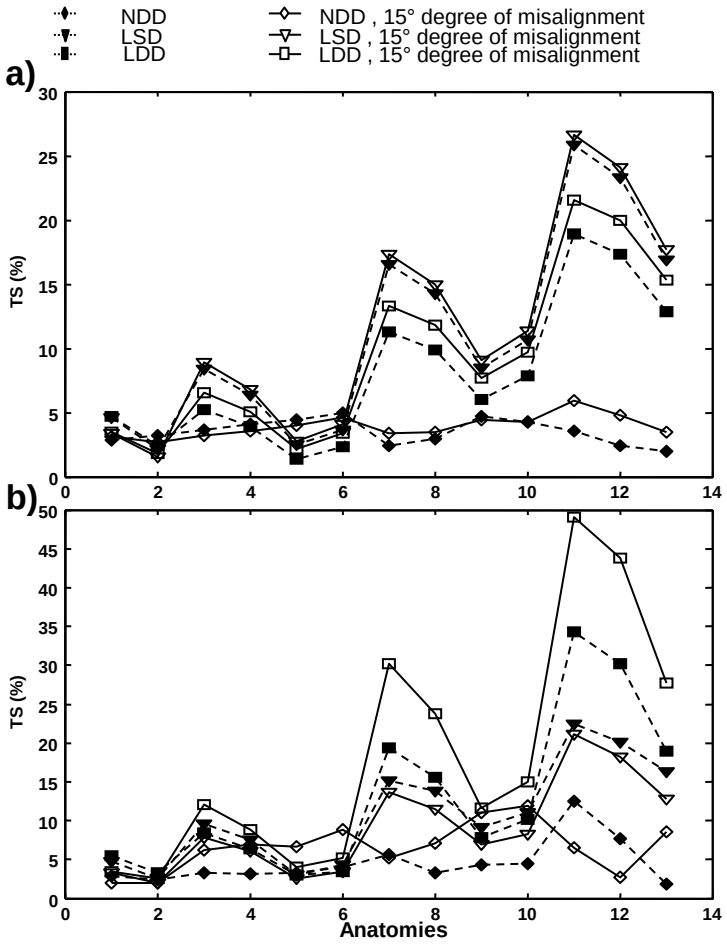
NDD
LSD
LDD
NDD , 15° degree of misalignment
LSD , 15° degree of misalignment
LDD , 15° degree of misalignment
a)
b)
TS (%)
TS (%)
Anatomies

Fig 6

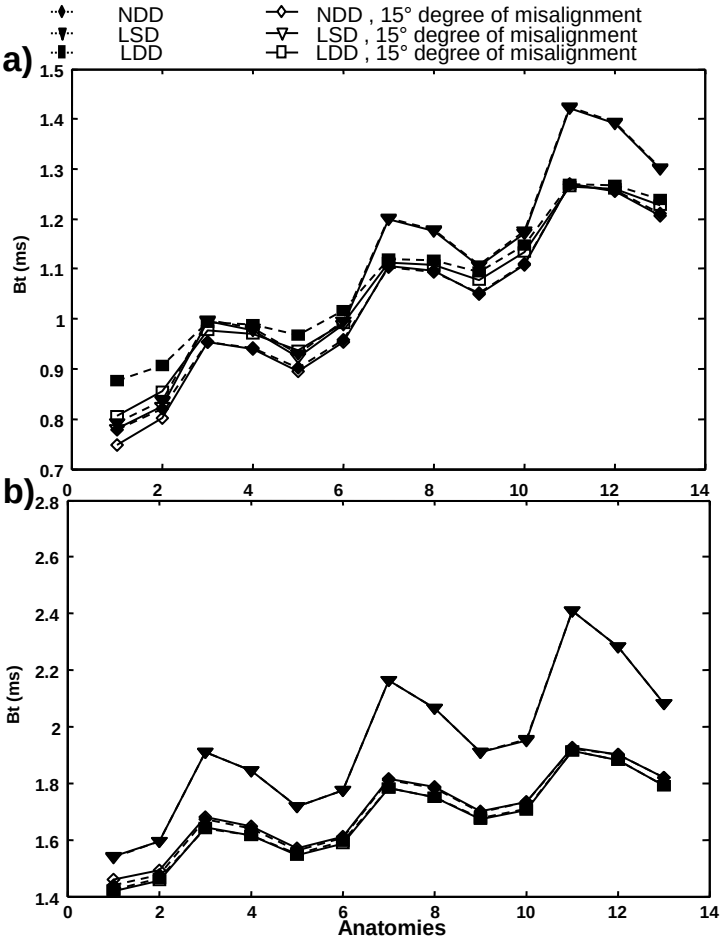
NDD
LSD
LDD
NDD , 15° degree of misalignment
LSD , 15° degree of misalignment
LDD , 15° degree of misalignment
a)
b)
Bt (ms)
Bt (ms)
Anatomies